Landslides (2016) 13:39–54
DOI 10.1007/s10346-014-0553-2
Received: 22 August 2014
Accepted: 30 December 2014
Published online: 14 January 2015

Jia-wen Zhou · Peng Cui · Ming-hui Hao

Comprehensive analyses of the initiation and entrainment processes of the 2000 Yigong catastrophic landslide in Tibet, China

Abstract The 2000 Yigong landslide was one of the most catastrophic landslides worldwide, resulting in huge casualties and property losses. The dynamic process of the Yigong landslide was very complicated, especially for the initiation and entrainment mechanism during the landslide movement process. The topography, geological condition, traces left by the landslide, and distribution characteristics of the landslide deposits were determined by field investigations, combined with several years of monitoring the temperature and rainfall data in this region. The initiation mechanism of the Yigong landslide is presented. The main reasons for the landslide initiation are as follows: the strength reduction of rock masses (especially for the weak structural surface), the impact from years of freeze-thaw cycles, the superposition of glacier melting and heavy rainfall on the slope, and a slope that was almost at the limit state before the landslide. Laboratory tests and physical modeling experiments were carried out to study the entrainment process of this landslide. Combined with the topographic survey data and theoretical analyses, the entrainment mechanism during the movement process of the Yigong landslide is presented. The old landslide deposits on the lower slope collided with and were scraped by the high-speed debris avalanche, which resulted in the volume amplification of the landslide. The existence of water plays a key role during the landslide initiation and movement processes.

Keywords Yigong landslide · Dynamic process · Initiation mechanism · Entrainment · Water

Introduction

Rapid catastrophic landslides, often defined as having a minimum volume of 10^6 m^3, can cause huge property loss and human death because of their large volume and high speed (Korup et al. 2007; Kuo et al. 2013; Pudasaini and Miller 2013; Weidinger et al. 2014). Previous studies have shown that in recent years, the occurrence frequency of rapid and long-runout catastrophic landslides has significantly increased because of the changes of global climate, such as rising temperature, heavy rainfall, and retreating snowline (Crosta et al. 2009). Catastrophic landslides are widely distributed worldwide, especially in the mountainous regions, such as the southwest of China (Wang et al. 2013). On 12 May 2008, the great Wenchuan earthquakes resulted in many catastrophic landslides and provided rich data to study the dynamic problem of rapid giant landslides (Huang and Li 2009; Tang et al. 2010; Dai et al. 2011; Yin et al. 2011; Zhou et al. 2013a). The initiation mechanism and motion process are very important to understand the dynamical process of giant landslides, which can provide possible preventive measures for potential giant landslides.

Landslides and other slope failures can be triggered by different factors, such as earthquakes, heavy rainfall, freeze-thaw cycles, glacier melting, and human activities (Evans et al. 2001). The initiation mechanisms of landslides under different triggering factors are not the same and are also influenced by the geological condition of the slope (Acharya et al. 2011). Triggering factors for the landslide can be divided into two main types: long-term factors, such as freeze-thaw cycles, weathering, and unloading, and short-term factors, such as strong earthquakes and heavy rainfall (Barth 2014). Most of the catastrophic landslides are triggered by the strong earthquake, such as the Tangjiashan landslide, the Donghekou landslides, the Wenjiagou landslide, and the Daguangbao landslide triggered by the 2008 Wenchuan earthquake (Yin et al. 2011) and the Tsaoling landslide triggered by the 1999 Chi-Chi earthquake (Tang et al. 2009). Because strong earthquake poses huge energy on the slopes in the earthquake hit area, some of the catastrophic landslides are triggered by heavy rainfall, for example, on 9 August 2009, a catastrophic landslide (Hsiaolin landslide) is triggered by the accompanying heavy rainfall from Typhoon Morakot in Kaohsiung County, Taiwan (Lo et al. 2011). Previous studies have pointed out that water content within the sliding mass and the sliding bed can accelerate rock mass dilation and fragmentation and a successive increase in mobility (Crosta et al. 2009). Landslides may be initiated by one triggering factor or several coupling factors. Furthermore, the failure of the slope is controlled by internal factors, such as terrain condition, mechanical properties of the rock mass, and distribution of joints and structural surface; the failure mode and probability for different slopes are not the same (Mather et al. 2014).

During the motion process of rapid giant landslides, the rapid sliding masses will interact with the bed materials along the traveling paths, especially for the saturated accumulations (Legros 2002; Dufresne 2012). The high-speed sliding mass can entrain large volumes of sediments both in a dry state and a saturated state (Angeli et al. 1998; Dufresne and Davies 2009). Entrained dry material is generally the consequence to reduce the mobility of sliding mass (Crosta et al. 2009). However, according to the Xiejiadianzi catastrophic landslide triggered by the 2008 Wenchuan earthquake, Wang et al. (2013) have pointed out that an earthquake can simultaneously trigger liquefaction of runout path materials before the arrival of the landslide mass, thus greatly increasing the mobility of an overriding landslide. Entrainment of almost saturated material can have a more complex consequence, in which most can increase the runout distance, because of sudden undrained loading and impact on loose deposits, and entrainment of a saturated substrate can cause enhanced mobility (Crosta et al. 2009; Sassa 2000; Zhu et al. 2000). The bed materials are scoured and eroded by the sliding mass and mixed with the sliding mass and water, accreted to the main flow front or entrained, resulting in the change of the landslide form (Dufresne and Davies 2009; Lo et al. 2011). Some studies for rainfall-induced landslides have pointed out that high-speed sliding motion leads to grain crushing along the sliding surface, and the liquidated bed materials are

entrained by the upper sliding masses and finally resulted in the long-runout distance and increasing volume of sliding mass (Sassa 2000). The entrainment of sufficiently large volumes of bed materials and surface water in the traveling path can transform a dry rock avalanche into a debris avalanche/flow, which has greater mobility (Lv et al. 2003; McDougall and Hungr 2005). The volume of avalanches can be significantly increased through entrainment of a substantial amount of bed material during the movement process (Niemi et al. 2005). Here, field investigation, laboratory test, and theoretical analysis are used to study the initiation mechanism and entrainment process of the 2000 Yigong landslide.

Background

The 2000 Yigong catastrophic landslide occurred in the mountains of Tibet at 94° 58′ 03″ E, 30° 12′ 11″ N (Xu et al. 2012). The initiation zone of the 2000 Yigong landslide was located in Zhamu Creek, at the north side of the Yigong River, a tributary of the Yarlu River. In this section, the geomorphology and geological condition in the study area is briefly introduced, and then the main features of the 2000 Yigong catastrophic landslide are described.

Geomorphology

The 2000 Yigong landslide occurred in the steep high mountainous region, which is located on the southern flank of the Nyainqentanglha Shan Mountains in southeast Tibet (Shang et al. 2003). Figure 1a shows the location of the Yigong landslide area; the distance to Yigong Town is approximately 26 km, and the location is 50 km from Lulang Town and 95 km from Bomi City. An old dammed lake was formed on the Yigong River in 1900, and after 100 years, a new catastrophic landslide occurred in Zhamu Creek and also formed a huge landslide dam. Figure 1b shows the geomorphology condition of the Yigong landslide region.

As shown in Fig. 1b, the length of Zhamu Creek is approximately 9.7 km, with thick ancient glaciers and snow on the top slope when the slope elevation is greater than 4500 m. Bedrock is bared at an elevation of approximately 3100–4200 m, and large volumes of landslide deposits of outwash, glacial moraines, and others are accumulated at the lower slope and along Zhamu Creek. The total length of Zhamu Creek is approximately 10.6 km, the maximum elevation at the top creek is approximately 5515 m, and the minimum elevation at the lower creek of the Yigong River bed is approximately 2185 m, with a total elevation difference of 3330 m and a mean longitudinal inclination of 31.4 % (Xu et al. 2012). The 2000 Yigong landslide occurred at the top slope of Zhamu Creek; the elevation range of the initiation zone is approximately 4000–5515 m. Zhamu Creek is perpendicular to the Yigong River. When the landslide deposits rushed into the river, the water flow was blocked by the mixture of rocks and soils and formed a dammed lake.

Figure 2 shows the three-dimensional visualization of the Yigong landslide region. At the upper creek, the elevation is approximately 3800–5515 m, with the slope angle larger than 50° and side slope angles approximately 40°–50° (Hu et al. 2009a). The upper slope is mainly covered by thick glaciers. Slope failures occur easily under the special geomorphology conditions.

Figure 3a shows the steep terrain of the upper slope at the Zhamu Creek, and multiple glaciers cover the mountain top. At the middle creek, the elevation is approximately 2900–3800 m, with the slope angle approximately 15°–18° and side slope angles approximately 45°–80°. Large volumes of loose landslide deposits are accumulated in this section due to the effect of old slope failures, strong physical weathering, glacier melting, and other processes. At the lower slope, the elevation is approximately 2185–2900 m with a gentle slope inclination about 10°–15°. The outlet of the Zhamu Creek is the junction position with the Yigong River. Large amounts of landslide deposits are accumulated at this section due to the 1990 Yigong landslide in the same region (Yin 2011). Here, we select four terrain sections along the Zhamu Creek to analyze the terrain changes across the channel (the locations of the terrain sections are shown in Fig. 2).

As shown in Fig. 3a, erosions were strongly intensive at the upper slope; that means several landslides and collapses occurred in the same area in the past. According to the terrain data at different sections along the creek (Fig. 3b), we can find that the inclination for the slopes on both sides of the Zhamu Creek is very steep, while the width of the creek is relatively large at the upper section and gradually narrows with decreasing elevation. At the lower section of the creek, the terrain is flat and the width of the creek is enlarged. This special terrain condition will affect the motion of the landslide; part of the boulders may be blocked at the back of the narrowest location (Yin and Xing 2012).

Geology

In the study area, the rock masses at the slope surface are strongly weathered. Joints and fractures are well developed in the rock masses. The occurrences of the main joints in the study area include the following: (1) the dip direction of 328° and dip of 46.5°, (2) the dip direction of 120° and dip of 74°, (3) the dip direction of 64° and dip of 32°, (4) the dip direction of 180° and dip of 48°, and (5) the dip direction of 284° and dip of 72°. The layers of rock masses are also most consistent with the strike of the slope. The slope stability is controlled by the structural surfaces and rock layers. Wedge instability controlled by different structural surfaces is the typical slope failure mode in this region.

Under the effect of tectonic movements and geomorphic evolutions, the distribution of lithology in the Yigong landslide area is very complicated. The study area is located near the Gangdise batholiths (Xu et al. 2012). There are four main types of rocks in this area: granite, marble, sandstone or slate, and limestone, with different degrees of weathering and variability. Figure 4 shows four images of the different types of rocks in the Yigong landslide region.

At the upper section of Zamu Creek, the rock masses are mainly composed of granite and steep slate (Fig. 4a, c). Here, we emphasize that dolomite existed in the landslide initiation zone and deposition zone, with different weathering degrees (Fig. 4d). At the middle section, there are epimetamorphic rocks of the upper Pondo Group (C_{pn}) of the Carboniferous, including marble (Fig. 4b), sandstone, and slates interbedded with marbles (Shang et al. 2005). Large volume of loose landslide deposits also existed at the creek bottom in the middle section, mainly composed of fragmented gravels, sandy silt, and other debris. At the lower section, thick deposits from old rock avalanches or debris flows are accumulated.

During the field investigation process, a small number of the dolomites were weakly weathered; most of the dolomites were strongly weathered and transformed into white powder (Fig. 5a),

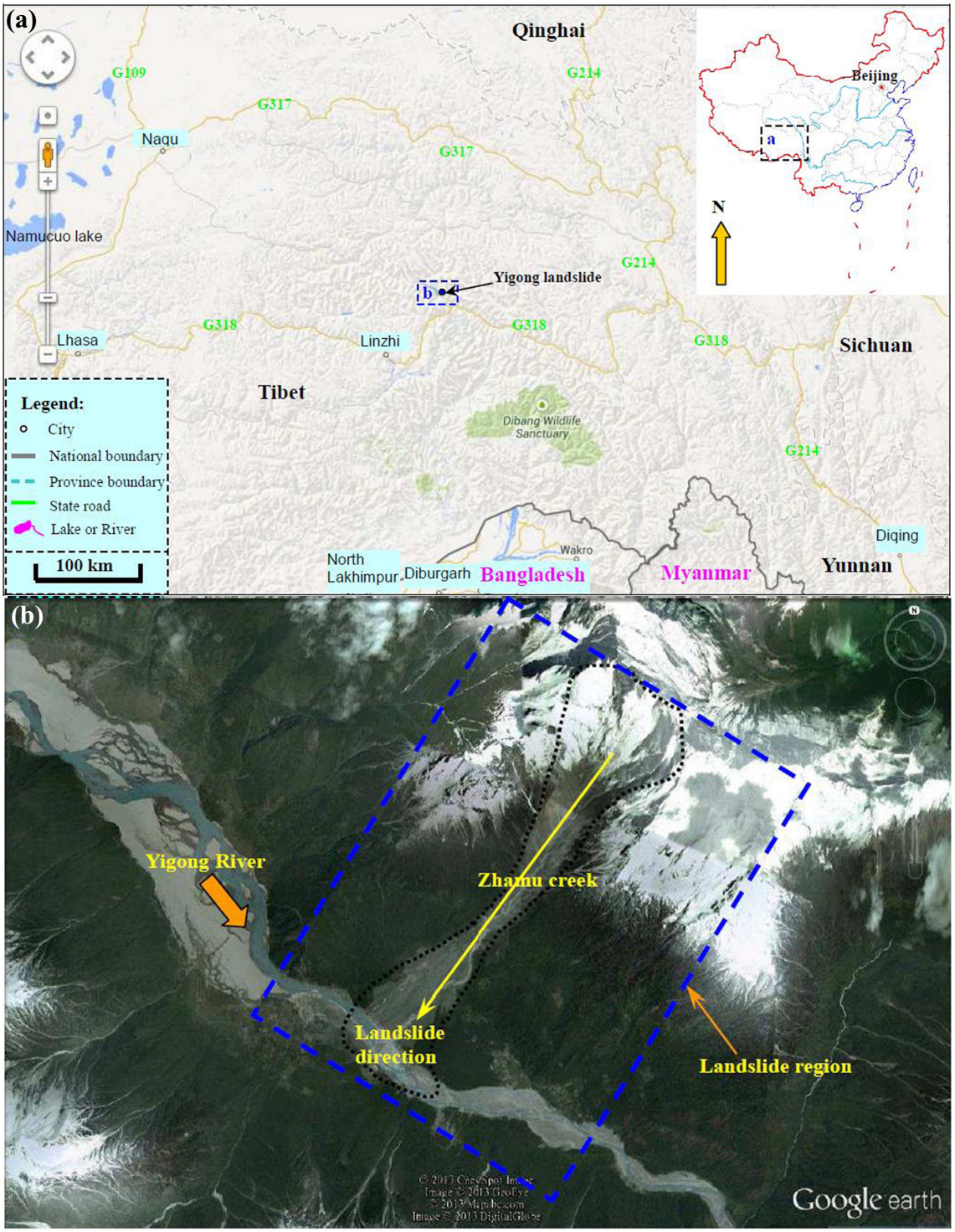

Fig. 1 **a** Location of the study area and **b** geomorphology condition of the Yigong landslide region (modified from Google Earth, 2014)

which is similar to lime but has more coarse particles and roughness. The powder of strongly weathered dolomite existed at different deposition locations, mainly at the middle section of landslide depositions. Figure 5b shows the X-ray diffraction analysis results for the sample of dolomite powder, and the mineral composition of dolomite is relative to a single of $CaMg(CO_3)_2$. The dolomite can be weathered more easily and significantly influenced by the freeze-thaw cycle, resulting in the decreasing of shear strength (Angeli et al. 1998; Borgatti and Soldati 2010).

The 2000 Yigong landslide

On 9 April 2000, a catastrophic landslide took place at Yigong, Southeastern Tibet, one of the largest non-seismic landslides in the world. Interpretation of remote sensing images shows that the

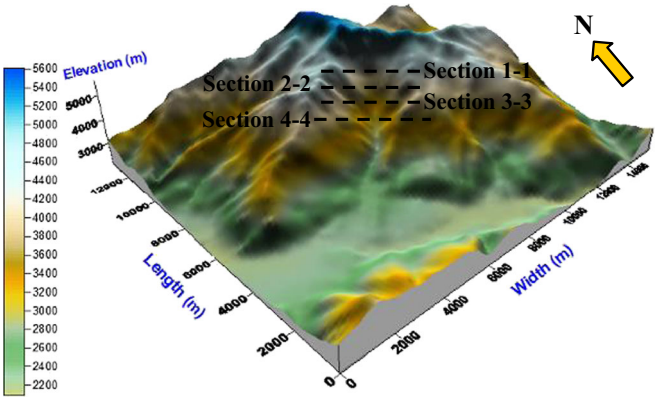

Fig. 2 Three-dimensional visualization of the Yigong landslide region (landslide region in Fig. 1)

total volume of the Yigong landslide deposits is approximately 3×10^8 m^3, while the accumulation area is approximately 6×10^6 m^2, and the average depth of depositions is approximately 50 m (Shang et al. 2003). The landslide was initiated at an elevation of approximately 5000 m (the volume of the landslide initiation region is estimated to be larger than 1×10^8 m^3) and then accelerated after a downward path of 1500 m because of the steep inclination of the slope. Rock fragmentations occurred in the rock mass because of the high motion speed and were then transformed into rock avalanche. The old deposits at the creek were impacted and scoured by the high-speed rock avalanche (which was mixed with ice blocks and water) and finally transformed into a super high-speed debris avalanche, eroding both banks of the creek (Xu et al. 2012). Finally, the debris avalanche was flushed into the Yigong River and formed a huge landslide dam. The landslide deposits are widely distributed at Zhamu Creek.

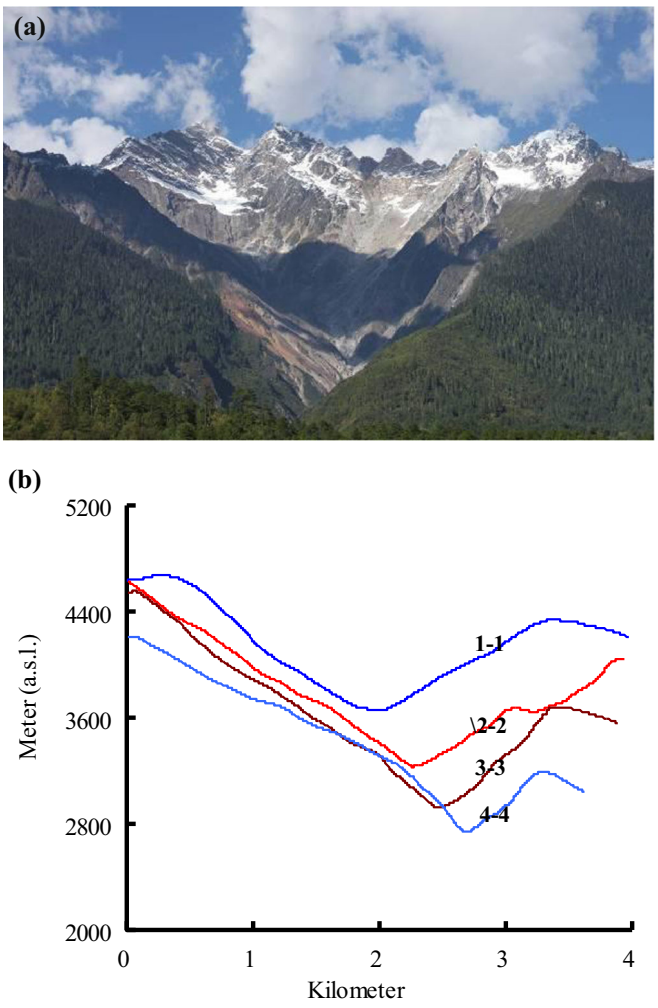

Fig. 3 Geomorphology features of the Zhamu Creek: **a** site photo and **b** terrain data at different sections along the creek (locations of the sections are shown in Fig. 2)

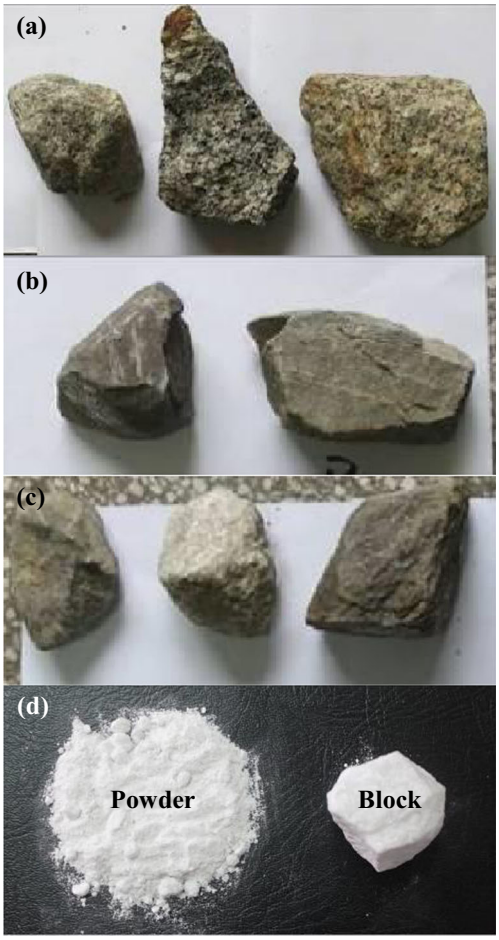

Fig. 4 Images of the different types of rocks in the Yigong landslide region: **a** granite, **b** marble, **c** slate, and **d** dolomite

Figure 6 shows the geological investigation results of the 2000 Yigong landslide. As shown in Fig. 6a, the 2000 Yigong landslide can be divided into three zones: the initiation zone, movement amplification zone, and deposition zone. The landslide was initiated at an elevation between 3800 and 5515 m and then ran into the amplification zone (which corresponds to the middle creek). The moving mass involved the scouring of loose debris on both banks and the bottom at a high speed. Figure 6e shows the main geological profile for the location of A–B; we can see clearly that the slope gradually decreased during the motion. When the moving mass attained the narrow location of the creek, the moving mass became thicker and some boulders were blocked here.

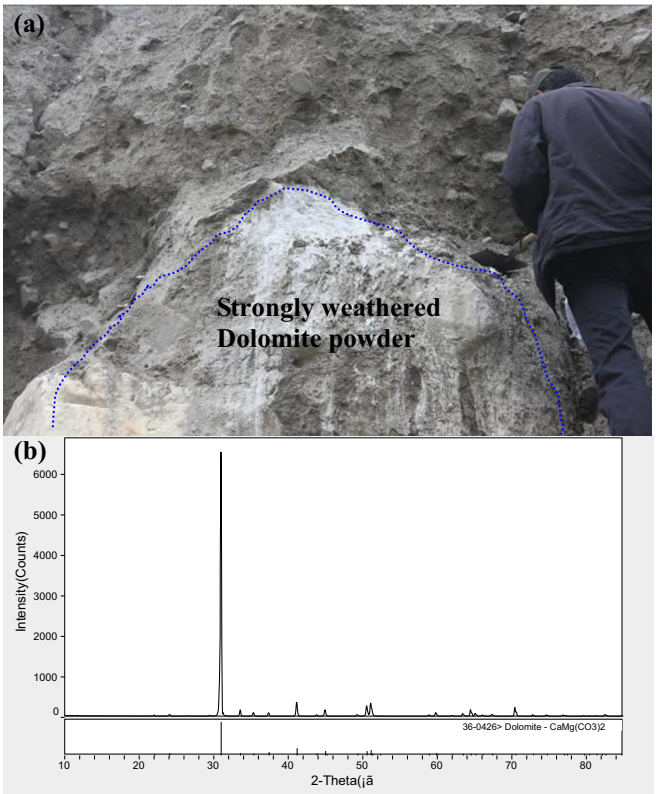

Fig. 5 **a** Powder of strongly weathered dolomite and **b** X-ray diffraction analysis for the sample of dolomite powder

From the field investigation results, we can determine the material compositions at different locations: (a) at the tail of deposition zone, the deposition height is approximately 4–10 m (Fig. 6b) and the landslide deposits are mainly composed of boulders with a proportion of approximately 70–90 %; (b) at the middle of the deposition zone, the deposition height was approximately 35–65 m (Fig. 6c) and the landslide deposits are mainly composed of rock debris, sandy silt, and solitary stone; the proportion of sandy silt is approximately 40–60 %; and (c) at the lower of deposition zone, the deposition height is approximately 50–80 m (Fig. 6d) and the landslide deposits are mainly composed of rock debris and sandy silt; the proportion of sandy silt is approximately 50–70 %. At the middle and lower deposition zones, the new 2000 landslide deposits covered the old 1900 landslide deposits. Figure 7 shows the distribution of the landslide deposits for the 2000 Yigong landslide.

As shown in Fig. 7(a), the deposition of the 2000 Yigong landslide can be divided into three zones: (1) the boulder deposition zone, (2) the debris and sandy silt deposition zone, and (3) the impact and scouring zone. As shown in Fig. 7(b), at deposition zone 2, the landslide deposits are composed of two main types of material: rock debris and soils. Three-layered structural characteristics existed in the lower deposition zone (from one eroded section) because of the high mobility of the debris avalanche. The top layer is the new 2000 landslide deposit, and the lower layer is the old 1900 landslide deposit interbedded with an overconsolidated layer (which is mainly composed of fine particles). At the tail of the landslide deposits region, boulders accumulated (Fig. 7(c)) and several giant stones exist in this region, which belong to the landslide deposition zone 1. During the motion process of debris avalanche, the old depositions were scoured and entrained by the moving mass, due to the high speed of the moving mass and steep terrain of Zhamu Creek.

Initiation mechanism of the Yigong landslide

In this section, combined with the geomechanical analysis and long-term monitoring data of temperature and rainfall, the initiation mechanism of the 2000 Yigong landslide is presented.

Geomechanical analysis of slope

At the initiation zone of the 2000 Yigong landslide, steep slate and granite are the main rock masses. The spacing of the slate is approximately 1.0–5.0 m, and under the effect of the upper weight of the rock mass and thick glacier, toppling and bending failure occurred to the slate during a long geological history. The bending failure surface can provide a potential sliding surface for the initiation of landslides. The slope stability of the initiation zone is controlled by the structural surfaces. Figure 8 shows the typical geological condition of the initiation zone for the 2000 Yigong landslide.

As shown in Fig. 8(a), there are five joint sets in the landslide initiation zone; the occurrence parameters of those joints are as follows: (1) in joint set 1, the dip is approximately 40–50° and the spacing is approximately 1.5–3.0 m; (2) in joint set 2, the dip is approximately 70–80° and the spacing is approximately 0.5–1.5 m; (3) in joint set 3, the dip is approximately 25–35° and the spacing is approximately 0.5–1.5 m; (4) in joint set 4, the dip is approximately 70–80° and the spacing is approximately 2.0–5.0 m; and (5) in joint set 5, the dip is approximately 30–55° and the spacing is approximately 1.5–4.5 m. The landslide initiation zone can be divided into three subzones: (a) a tensile failure surface at the tail of the slope (zone 1), in which a clearly fractured surface can be seen; (b) a dislocation layer with several rock layers along the direction of slate (zone 2); and (c) a compound weak layer (zone 3). The upper part is a weak layer of bending failure surface of slate (rough), and the lower part is a rock layer (smooth). To the left of subzone 1, clearly bending failure surface existed and an old landslide occurred in this area (Fig. 8(b)). The 2000 landslide initiation zone is a typical wedge failure mode, which is controlled by two structural surfaces and a tensile failure surface, and a free surface at the slope front provided the potential initiation of the landslide in this region.

Furthermore, thick glaciers covered the slope rock masses and could have resulted in three adverse impacts on the landslide initiation zone: (1) an increase in the weight of the sliding mass, (2) the melting and freezing of the glacier effect on the rock masses or structural surfaces such as the unloading-loading cycle for rocks, and (3) the melting water could decrease the shear strength of the structural surface and increase the pore water pressure in the slope rock masses. The typical geological condition on the top slope provides favorable conditions for the initiation of landslides. The variation of the external environment condition on the slope can be summarized in two aspects: decreasing shear strength and increasing stress.

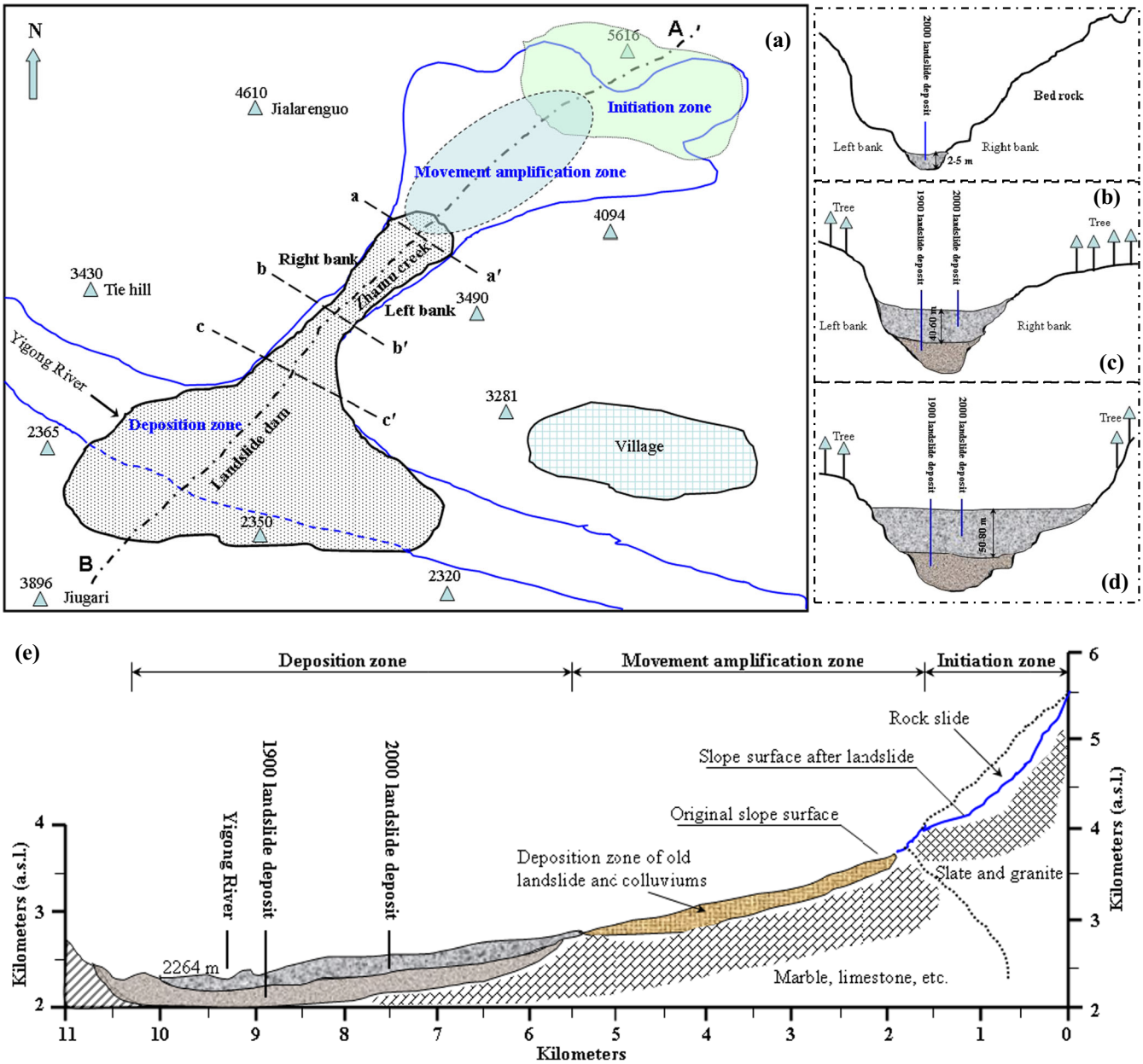

Fig. 6 Geological investigation results of the 2000 Yigong landslide: **a** overview of the landslide motion and deposition zone, **b** cross section *a*–*a*′, **c** cross section *b*–*b*′, **d** cross section *c*–*c*′, and **e** main geological profile for the location of A–B

Effect of temperature changes

In the study area, the 1951–2011 data recorded by the Yigong Meteorological Station shows that the average temperature was approximately 8–10 °C. Since the 1970s, the temperature in this area has had a slowly rising tendency with a total ratio of 0.3 °C/10 years (Shang et al. 2003). Figure 9 shows the monitoring results of temperature in the study area.

As shown in Fig. 9a, the average temperature gradually increased during 1 March to 4 May, which means that the melting of glacier and snow gradually increased during this season. However, there was no significant difference between the years 1998, 1999, and 2000. Along with the rises of temperature from April to May, glaciers and snow cover melt and water flow was generated in Zhamu Creek. The water flow not only affects the loose landslide deposits located at the creek but also influences the slope stability in this region. As shown in Fig. 9b, the daily temperature difference is the difference between maximum temperature and minimum temperature in 1 day. The daily temperature difference in the study area was relatively large; the average value was approximately 12.5 °C from 1 January 2000 to 1 January 2001, and the maximum value attained was 26 °C. The temperature difference from 1 April to 15 April 2000 was relatively large, which had a significant effect on the initiation of landslide on 9 April 2000. Temperature changes can provide two aspects for the initiation of landslides: (a) a freeze-thaw cycle on structural surfaces and (b) glacier melting resulted in the decreasing of shear strength and increasing pore water pressure.

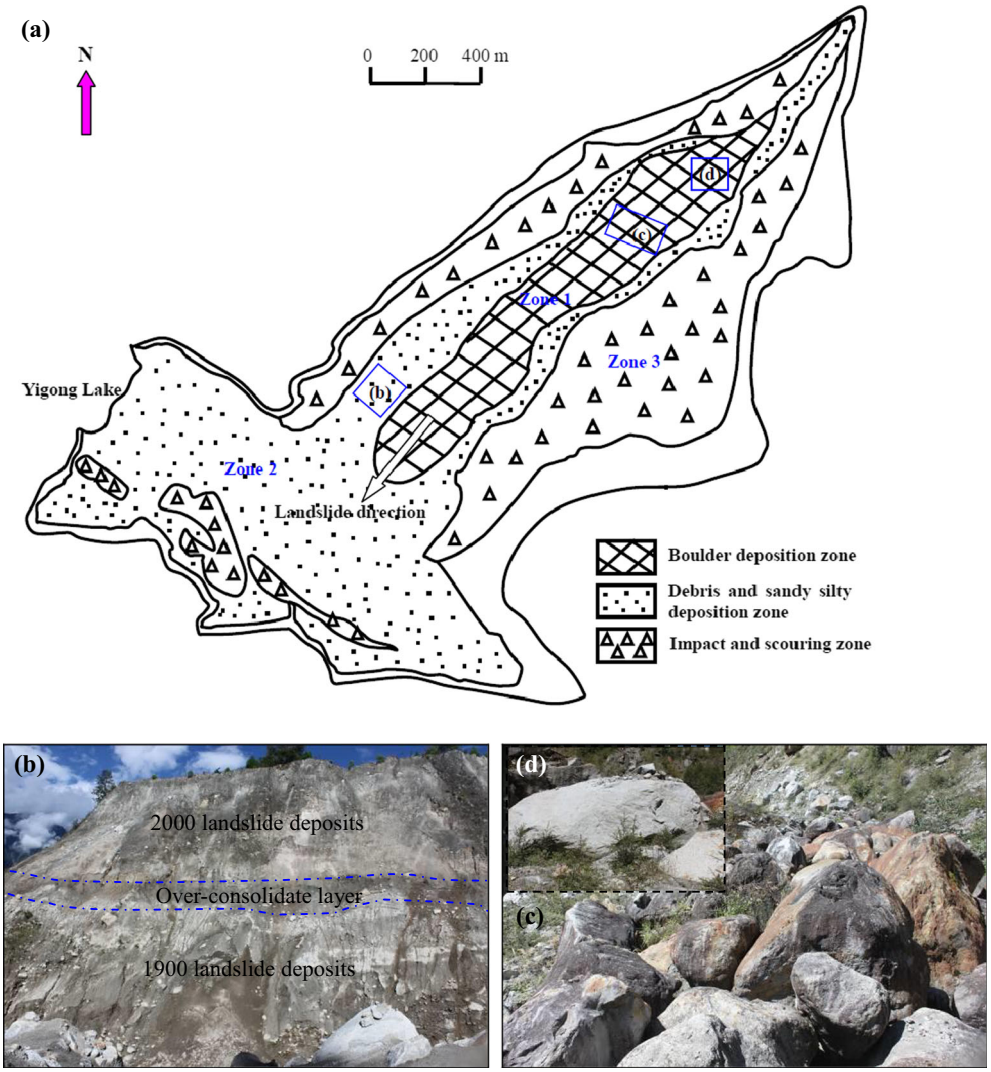

Fig. 7 Distribution of the landslide deposits for the 2000 Yigong landslide: *a* partition of deposition zone (Xu et al. 2012, modified), *b* site photo taken at the lower deposition zone, *c* site photo taken at the upper deposition zone, and *d* giant stone at the tail of landslide deposits region

There are two types of freeze-thaw cycles for the rock mass in this area: the seasonal freeze-thaw cycle (with a period of 1 year) and the daily freeze-thaw cycle (with a period of 1 day). Figure 10a shows the temperature monitoring result from 1 January 1996 to 30 December 2003, and Fig. 10b shows the temperature monitoring results from 15 March to 16 April 2000.

As shown in Fig. 10a, the annual temperature variation periodically changes; the minimum temperature (about −5 °C) occurred in December or January and then gradually rose to the maximum temperature (approximately 20 °C) in June or July. This long-term freeze-thaw cycle resulted in the gradual decreasing of shear strength of rock masses and structural surfaces. As shown in Fig. 10b, the freeze-thaw cycle property of daily temperature is exhibited. However, strong cycles did not occur because the daily temperature variation was disordered. The mechanical properties of rock masses were also influenced by the daily freeze-thaw cycle.

Previous studies have shown that freeze-thaw cycles have a significant influence on the mechanical properties of rocks, including porosity, compressive strength, elastic modulus, and shear strength (Ma et al. 1999). Microcracks and micro-defects occur in the rocks, and water will run into the rocks. The water in the rocks begins to freeze when the temperature is lower than 0 °C. Volumetric expansion occurs during the freezing process and leads to microcrack propagations in the rock. Local damage occurs in the rocks and results in the decreasing of compressive strength and shear strength (Draebing et al. 2014). However, the ice in rocks melts when the temperature is greater than 0 °C, while pore water pressure is formed in the rocks, and also results in the decreasing of shear strength (Zhu et al. 2011; Krautblatter et al. 2013). With the increasing numbers of freeze-thaw cycles, the shear strength of rock masses or structural surface is gradually decreased (Lai et al. 2010). The freeze-thaw cycle not only decreases the shear strength of rock masses but also results in the increasing stress distribution in the slope and finally causes the initiation of landslides in high mountainous regions (Bayard et al. 2005).

Effect of rainfall

According to the 1951–2011 data from the Yigong Meteorological Station, the mean annual rainfall in the Yigong area was

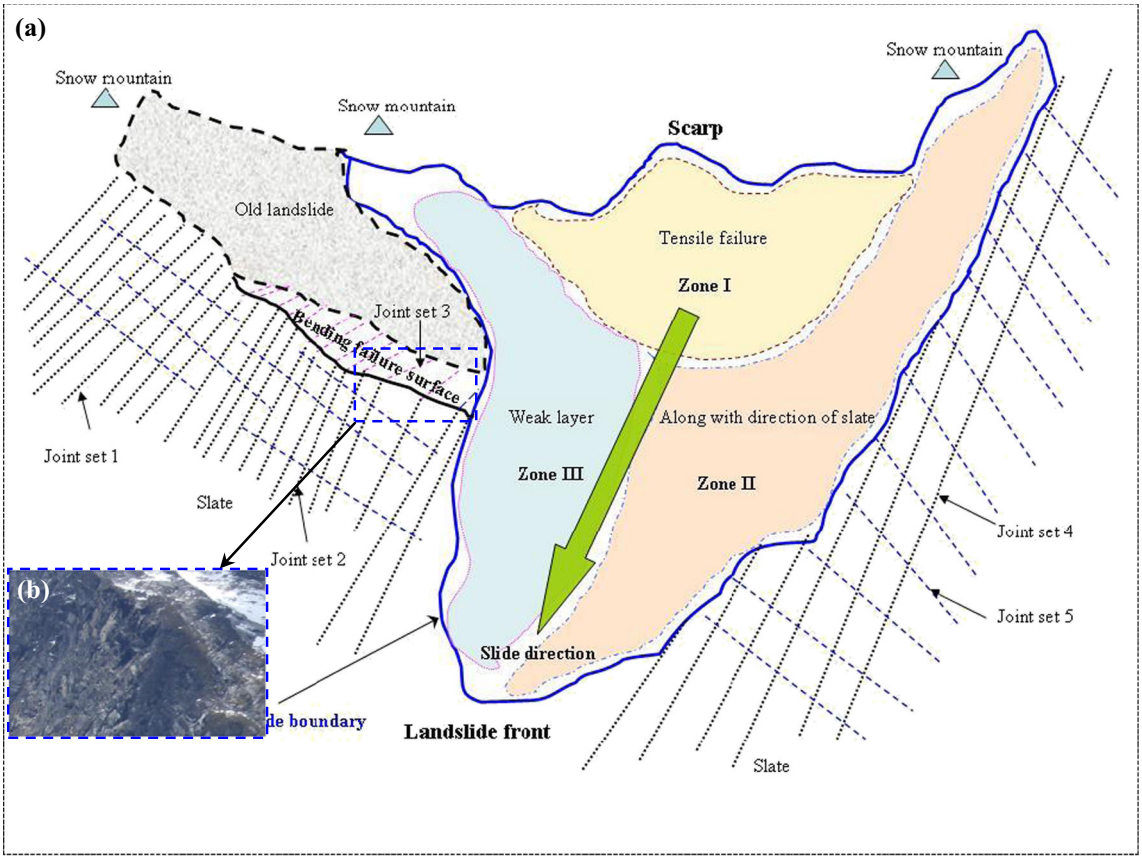

Fig. 8 Typical geological condition of the initiation zone for the 2000 Yigong landslide at the top of Zhamu Creek

approximately 810–1250 mm. The rainfall from April to October accounts for 90 % of the annual total rainfall, and November to February is the dry season (Shang et al. 2003). Figure 11 shows the rainfall monitoring results in the Yigong region.

As shown in Fig. 11a, most of the daily rainfall is approximately 0–40 mm, but some heavy rainfall occurred on special days. The maximum daily rainfall occurred on 20 October 1998, approximately 111.7 mm. The daily rainfall was not distributed uniformly during the whole year; the daily rainfall during the rainy season was greater than during the dry season. The rainfall in different seasons has similar characteristics. The rainfall data are monitored in the valley region, and the rainfall level at the top of the mountain is greater. Thus, in the initiation zone of Yigong landslide, the rainfall is relatively abundant. Figure 11b shows the comparison results for the monthly rainfall of 1998, 1999, and 2000. We can see that rainfall occurred mainly during April to October. On April, the monthly rainfall in 2000 was approximately 175 mm, more than the years 1998 (38 mm) and 1999 (80 mm). Increasing rainfall on April 2000 played some key effects on the initiation of the 2000 Yigong landslide. Figure 12 shows the daily rainfall during 1 March to 4 May 2000 at the study area.

As shown in Fig. 12, in 2000, when the recent Yigong Landslide occurred, the rainfall from April 2 to April 9 was more than 60 mm (Hu et al. 2009b) and the total rainfall in April was approximately 175 mm, 90–135 % more than the mean value from the same period in southeast Tibet (Liu 2002). The daily rainfall on 9 April 2000 was approximately 25 mm. The abundant rainfall resulted in the saturation of loose landslide deposits at Zhamu Creek and increasing pore water pressure in the upper slope, especially in the structural surfaces. Furthermore, relatively more water flow formed in Zhamu Creek, which could have affected the motion of debris avalanche.

Comprehensive analysis

Through the above analyses of the geological and environmental conditions at the Yigong area, we found that the main reasons for the initiation of the 2000 Yigong landslide were typical slope geological conditions, temperature changes, and heavy rainfall on April 2000.

Table 1 summarized the annual environment conditions at the Yigong area from 1991 to 2001, including temperature and rainfall. Extreme maximum temperatures always occurred from June to August, with values of approximately 29 to 31 °C. However, the extreme minimum temperatures always occurred from December to February, with values of about −10 to −13 °C. The maximum rainfall for the whole year of 2000 occurred on 9 April.

The reasons for the initiation of the 2000 Yigong landslide are the coupling of long-term effects and short-term impact. Regarding the long-term effects, there are two aspects, as mentioned above: (a) the loading-unloading cycle on the rock masses or structural surfaces due to the melting and freezing of glaciers and (b) the continuous seasonal and daily freeze-thaw cycles on the rock masses or structural surfaces. These two aspects resulted in the gradual decrease of mechanical properties of rock masses or

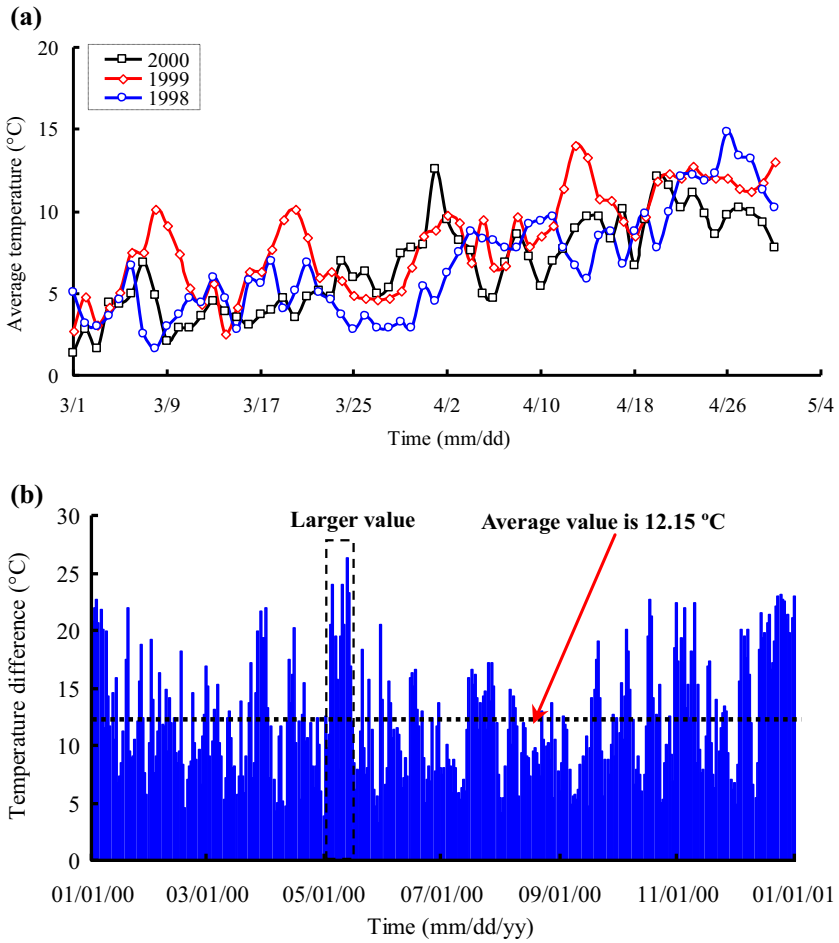

Fig. 9 Temperature monitoring results in the study area: **a** comparison analysis for the average temperature during 1 March to 4 May in 1998, 1999, and 2000, and **b** daily temperature difference from 1 January 2000 to 1 January 2001

structural surfaces, including compressive strength, porosity, and elastic modulus, especially for the shear strength of rock masses or structural surfaces. Furthermore, the tensile fracture has gradually been increasing over a long period. Other long-term factors including weathering and unloading can also have adverse impacts on the slope stability.

Regarding the short-term effects, the rising temperature will accelerate the melting of glacier and snow; by coupling with heavy rainfall, the water content of the structure surface is increased sharply and results in a larger decreasing of shear strength. The heavy rainfall and melting of glacier and snow also resulted in the increasing of pore water pressure on the structural surfaces. Another key factor for the initiation of the landslide is the special geological conditions of the upper slope at Zhamu Creek. The potential sliding wedge is controlled by two structural surfaces and a tensile failure surface, which are sensitive to temperature change and water content.

Regarding the initiation mechanism of the 2000 Yigong landslide, special geological conditions at the top slope provide necessary conditions for the initiation of the landslide. Long-term freeze-thaw and loading-unloading cycles resulted in the gradually deterioration of the slope stability. The direct triggering factors are short-term heavy rainfall and rising temperatures on April 2000. The increasing water content and pore water pressure in the structural surface finally resulted in the catastrophic landslide in the Yigong area in 2000.

Entrainment effect during motion process

For the 2000 Yigong landslide, the volume of landslide deposits was about three times the volume of initiation the zone. The entrainment effect during the motion process obviously occurred because of the high motion speed and water flow.

Motion of high-speed landslide

The entrainment of path material is an important feature of many rapid landslides (Hsü 1978; Evans et al. 2001; Dufresne et al. 2010). During the motion process of rock avalanches, the landslide paths are typically covered by thick surficial deposits. These deposits may be loose and have high water content. The rapid loading due to the weight and momentum of the moving masses may cause failure and mobilization of these bed materials and resulted in the volume amplification of the landslide (Scott et al. 2005; Cepeda et al. 2010). Figure 13 shows the topography changes for the main geological section of Zhamu Creek before and after 2000 Yigong landslide, which is extracted for the high-resolution digital elevation model of the study area.

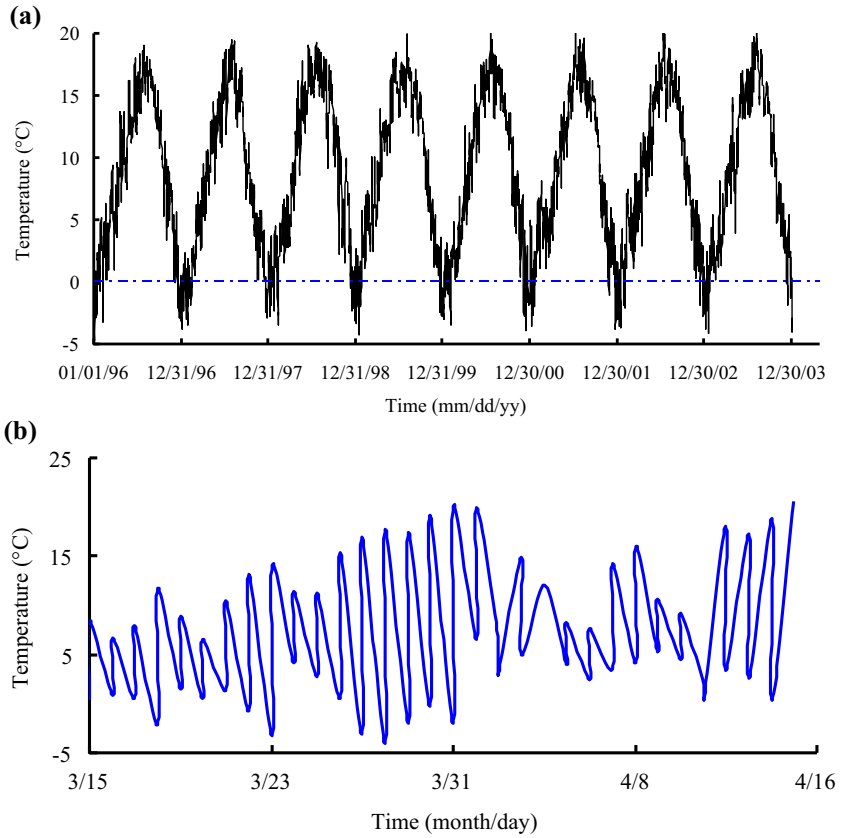

Fig. 10 Different freeze-thaw cycles for the rock mass in the study area: **a** seasonal type and **b** daily type

As shown in Fig. 13, many loose surficial deposits were covered on Zhamu Creek during the motion process of the high-speed rock avalanche, and these bed materials were scoured and eroded by the sliding masses, which finally resulted in the volume amplification of the landslide. The serious scouring of the bed materials at the middle section of Zhamu Creek by sliding masses can clearly be seen.

Laboratory tests

Regarding the entrainment problem of high-speed landslides, a simple laboratory test was carried out to study the bed materials impact and scouring by the sliding masses. Figure 14 shows the experimental equipment for the laboratory tests. The horizontal length of the flume is 2.0 m, the height is 1.5 m, and the width is 0.3 m. Loose bed materials are accumulated at the lower of flume, and the sliding mass (composed by rock blocks) are placed in the topper of flume (Fig. 14b). These experiments are solely conceptual since no scaling calculations were done. Table 2 shows the experimental design for the impact and scouring effect on the bed materials.

As shown in Table 2, 11 tests under different material compositions and weight ratios, with and without water, were carried out. The weight ratio is a key factor affecting the motion distance of bed materials. Figure 15 shows the movement distance of bed materials influenced by the weight ratio between sliding mass and bed depositions.

As shown in Fig. 15, these test results were obtained under dry conditions, without water flow. The movement distance of bed materials increased with the weight ratio between sliding mass and bed depositions, an approximately linear relationship. During the landslide motion process, the bed depositions are impacted and scoured by the sliding masses (Van Wyk de Vries et al. 2001; Crosta et al. 2005; Dufresne 2012). A larger weight ratio between the sliding mass and bed deposition means the difference of impact energy and friction resistance is increased, resulting in the longer movement distance of bed materials. Figure 16 shows the experimental results for the impact and scouring of sliding masses.

As shown in Fig. 16a, rock blocks were used to simulate the rock avalanche and placed at the top of the flume and the loose deposits were covered on the lower flume with a uniform thickness. Figure 16b shows the final deposited situation of test No. 6 under dry condition, and the W_R is 1.0. The bed depositions were impacted and scoured by the moving mass, and the total motion distance of the bed materials was 16.0 cm. Most of the rock blocks were blocked at the tail of landslide deposits, and some blocks moved to the front of the flume. When water flow was added in the experimental process, the bed depositions were saturated, pore water pressure formed in the soils, and the friction resistance of the bed materials decreased sharply. When the sliding mass impacted on the bed materials, the huge impact energy and excess pore water pressure resulted in the failure and scouring of bed materials. Then, the bed loose deposits were mixed in the sliding

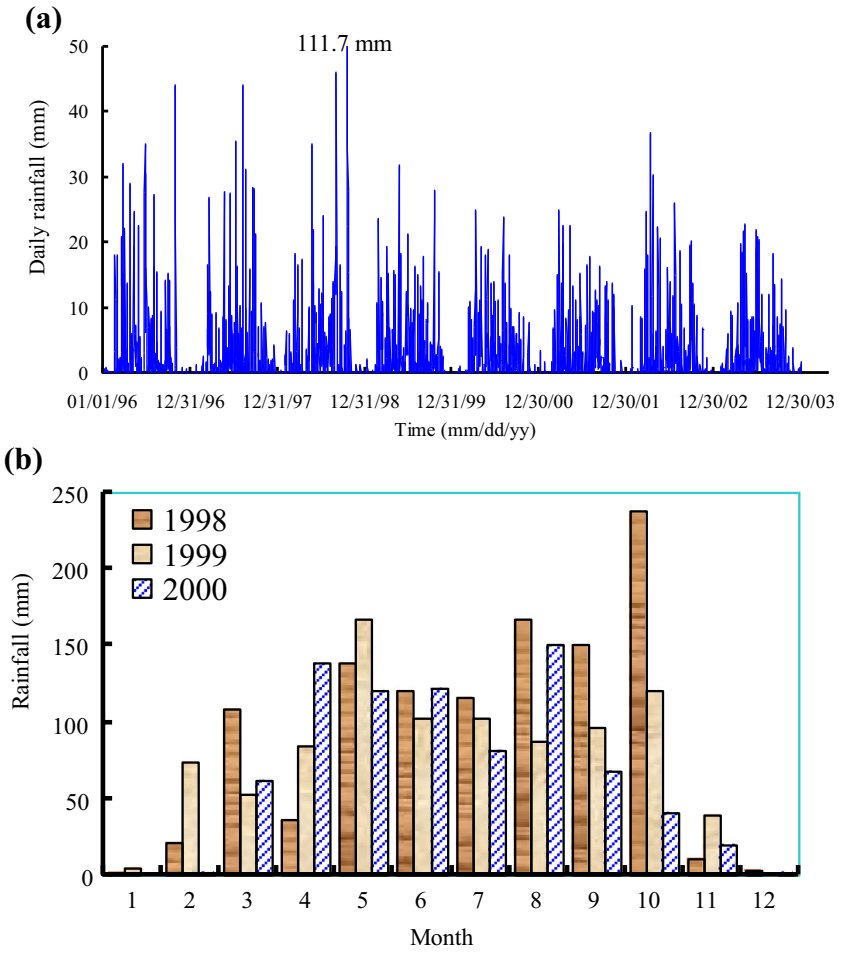

Fig. 11 Rainfall monitoring results in the Yigong region: **a** daily rainfall during the years 1996–2003 and **b** monthly rainfall for the years 1998, 1999, and 2000

mass and moved down along the flume. The final deposited situation of test No. 4 is shown in Fig. 16c. The motion distance of the bed materials is larger than the dry condition, approximately 43.8 cm. Compared with the actual deposited situation in Fig. 7a, the experimental deposited situation has the same distribution characteristics as the actual landslide. The impact and scouring of bed materials resulted in the volume amplification of the sliding mass.

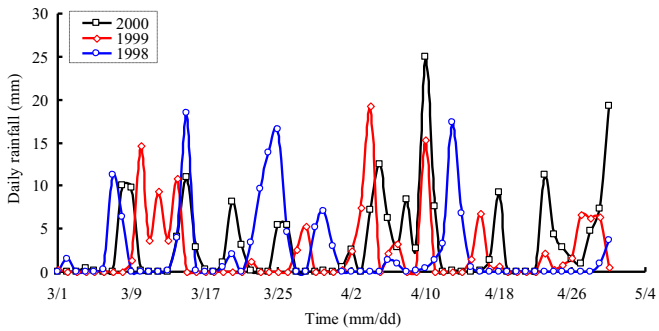

Fig. 12 Daily rainfall during 1 March to 4 May 2000 at the study area

Movement amplification effect

From the field investigation and above analysis results, the dynamical process of the 2000 landslide can be summarized as follows: landslide initiation (wedge failure)→acceleration and fragmentation→rock avalanche→scouring and entrainment→debris avalanche→landslide deposition, as shown in Fig. 17a. The landslide was initiated under heavy rainfall and rising temperature at the top slope of Zhamu Creek, with a wedge failure type. Then, the sliding mass moved down the steep terrain and attained a high speed. The sliding mass was fragmented by the effect of strike, collision, and other impact loading, and then, the sliding mass transformed into a rock avalanche. During the motion process of the rock avalanche, much bed deposit was impacted and scoured by the sliding mass. This situation became more serious because the water flow, the decrease in the shear strength of bed material, and the excess pore water pressure facilitated the failure. The failed bed material was mixed in the rock avalanche and moved with the sliding mass and resulted in the rock avalanche transforming into debris avalanche. When the sliding mass moved to the lower section of Zhamu Creek, a thin layer was formed between the new avalanche debris and the 1900 landslide deposits. The material composition of this layer is mainly water and fine particles, so that we can clearly see the three-layered

Table 1 Annual environmental conditions in the Yigong area from 1991 to 2011

Year	Average temperature (°C)	Extreme maximum temperature		Extreme minimum temperature		Annual rainfall (mm)	Maximum daily rainfall	
		Value (°C)	Time (dd-mm)	Value (°C)	Time (dd-mm)		Value (mm)	Time (dd-mm)
1991	8.6	28.8	22-Jun	−12.0	17-Jan	1128.5	43.8	2-Jun
1992	8.4	28.8	18-Jun	−13.7	24-Dec	714.2	43.1	24-Jun
1993	8.7	28.4	7-Jul	−12.6	29-Jan	810.0	26.5	28-Sep
1994	8.9	31.0	12-Jul	−12.1	23-Dec	847.3	36.9	10-Oct
1995	9.2	31.0	6-Aug	−13.0	28-Jan	1130.7	48.1	14-Jun
1996	8.9	28.3	21-Jul	−12.5	3-Jan	1068.4	44.1	29-Oct
1997	8.2	28.7	8-Aug	−12.7	19-Jan	930.6	44.1	9-Aug
1998	9.3	28.0	12-Jul	−10.8	9-Feb	1108.8	*111.7*	*20 Oct*
1999	9.4	30.2	1-Aug	−12.1	12-Jan	932.2	31.8	22-May
2000	8.8	29.2	25-Jul	−12.2	31-Jan	808.9	25.0	9-Apr
2001	9.1	31.2	8-Jul	−11.4	24-Dec	801.0	25.1	24-Mar
2002	9.1	30.2	9-Jun	−12.6	2-Jan	862.5	36.8	10-Apr
2003	9.1	30.0	7-Aug	−12.4	16-Jan	823.7	22.8	8-May
2004	9.0	29.3	6-Aug	−11.5	28-Dec	880.9	46.0	15-Apr
2005	9.6	28.6	15-Jun	−11.5	13-Jan	777.2	32.9	18-Apr
2006	9.8	31.2	17-Jul	−9.6	24-Dec	864.1	34.9	12-Sep
2007	9.7	29.4	13-Jul	−10.6	24-Jan	855.9	45.0	16-May
2008	9.1	29.1	12-Jun	−10.3	15-Feb	800.1	86.0	27-Oct
2009	10.2	30.9	20-Jul	−10.0	28-Dec	536.2	22.1	22-Feb
2010	9.6	30.7	15-Aug	−10.2	3-Jan	1080.6	39.3	11-May
2011	9.2	30.1	31-Aug	−9.2	16-Jan	838.7	44.8	25-Mar

structural characteristics of the landslide deposits (Fig. 7b). The middle layer is composed of over-consolidated materials and has a higher compression strength and lower porosity.

Figure 17 shows the whole dynamic process of the movement of the 2000 Yigong landslide. There are three types of entrainment modes for the high-speed landslide: impact, scouring, and erosion. When the rock avalanche attained the tail of the bed deposits, the entrainment of the sliding mass occurred through impact and scouring. The high-speed rock avalanche led to great impact energy on the bed materials and resulted in the failure of old

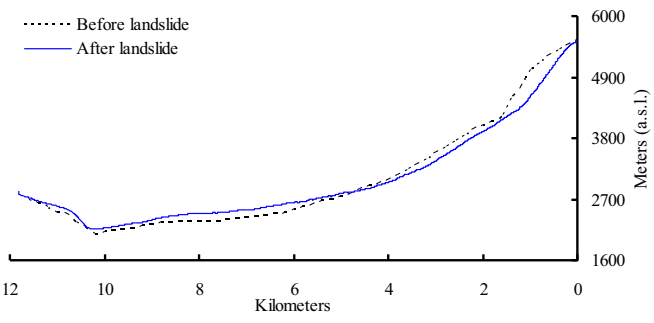

Fig. 13 Topography changes for the main geological section of the Zhamu Creek before and after the 2000 Yigong landslide

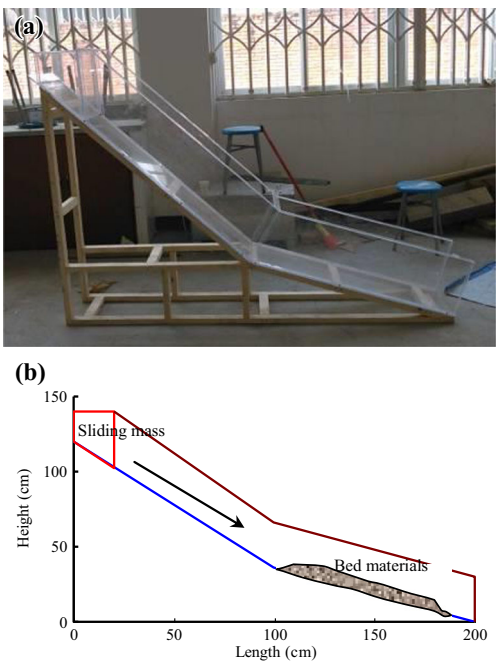

Fig. 14 Experimental equipment: **a** actual image and **b** size design

Table 2 Experimental design for the impact and scouring effect on the bed materials

No.	Depositions (kg)		Rock blocks (kg)	Water	W_R[a]	Motion distance (cm)
	<1 mm	2–5 mm	20–40 mm			
1	–	4.225	13.040	Y	3.1	72.3
2	–	6.235	11.560	Y	1.9	54.3
3	10.000	–	8.000	Y	0.8	11.6
4	3.000	5.000	12.000	Y	1.5	43.8
5	4.000	6.000	10.000	Y	1.0	23.0
6	4.000	6.000	10.000	N	1.0	16.0
7	4.000	6.000	4.000	N	0.4	2.5
8	4.000	6.000	8.000	N	0.8	11.0
9	4.000	6.000	12.000	N	1.2	28.0
10	4.000	6.000	15.000	N	1.5	46.0
11	4.000	6.000	20.000	N	2.0	58.0

Motion distance referred to the bed depositions

[a] The weight ratio between sliding rock blocks and bed depositions

deposits. Furthermore, during the motion process of the rock avalanche, the bed material was scoured by the sliding mass. This former entrainment process is shown in Fig. 17b. After the landslide initiation, the form and material composition of landslide varied during the whole motion process, and the cumulative volume of the landslide changed enormously along the path of movement. The path is described as a series of reaches that have a distinct morphology, width, and slope inclination, and the structural characteristics, material compositions, and mechanical properties are also not the same. These changes made the entrainment process of sliding mass very complicated.

As shown in Fig. 17c, the bed deposits were eroded by the high-speed sliding mass, especially when water flow occurred. The bed erosion at the base of the landslide is similar to bedload transport in fluvial hydraulics. The failure of bed material can be caused by the impact force and scouring effect and the generation of excess pore water pressures due to rapid undrained loading with possible liquefaction. The existence of water plays a key role during the motion process of landslides, especially for the entrainment of landslides.

In the Yigong area, the special terrain condition allowed the water flow to be easily collected in the Zhamu Creek. Heavy rainfall and glacier on April 2000 resulted in the saturation of bed deposits and larger water flow. During the motion process of the landslide, the landslide volume gradually increased through the entrainment effect and finally resulted in the volume amplification of the landslide deposits.

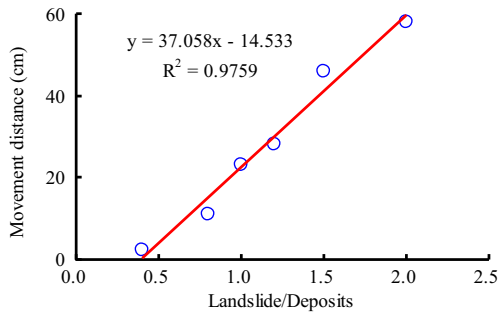

Fig. 15 Movement distance of bed materials influenced by the weight ratio between sliding mass and bed depositions

Discussion and conclusion

Discussion

The initiation mechanism and motion process of landslide are very complicated for the dynamical problem of high-speed landslides (Zhou et al. 2010). The initiation of landslides is not only influenced by the geological condition but also affected by the short-term environmental conditions, such as earthquake, heavy rainfall, or rising temperature (Wang et al. 2003; Tsou et al. 2011). Previous studies show that landslides may be initiated by some sudden events, such as strong earthquake, heavy rainfall, or rising temperature in a short time (Evans et al. 2001; Dai et al. 2011; Kuo et al. 2013; Barth 2014). However, heavy rainfall is not the single triggering factor for the 2000 Yigong landslides, and the rising temperature on April 2000 is another short-term triggering factor. Furthermore, the rock masses in a slope generally experienced a long-term geological evolution process, such as the tectonic effect, weathering and unloading, freeze-thaw cycles, and loading-unloading cycle. These long-term geological effects can result in the change of the slope stability state, including the decreasing of shear strength of rock masses and increasing of pore water pressure in slope (Zhou et al. 2013b). These reasons make the initiation mechanism of landslide very complicated under different conditions. However, one key issue should be emphasized here: the initiation of most landslides is a result of the coupling of long-term evolution and short-term effects on a slope.

Mass movement of the rock avalanche or debris avalanche is mainly influenced by the Lithology and topographical conditions. Fragmentation of rock masses and mobility of sliding masses are influenced by the lithology and its structural properties. For the 2009 Hsiaolin landslide, Lo et al. (2011) found that huge amounts of fragmented rock materials moved quickly downward and

Fig. 16 Experimental results for the impact and scouring of sliding masses: **a** experimental preparation, **b** final deposited situation of test No. 6, and **c** final deposited situation of test No. 4

transformed into a debris avalanche. Rock fragmentation can easily be happened during the motion process of high-speed landslide, part of the debris rushed over a high-level terrace and spread along the hillslope (Hungr et al. 2005). Special terrain condition plays a key role during the mass movement process. Regarding to the 2000 Yigong landslide, the sliding mass moved down the steep terrain with a high speed and then encountered the bed deposits. Huge impact energy is posed on the bed deposits, and a large volume of bed deposit was impacted and scoured by the sliding mass, resulting in the rock avalanche transformed into debris avalanche. Meantime, a part of the sliding masses are stopped and accumulated at the foot of the steep slope, because of the energy loss and the narrow terrain. The flat and straight topographical conditions along the runout path provide a favorable condition for the mass movement. The presence of water not only increases the mobility of sliding masses but also poses a great impact on the entrainment process during mass movement process.

For the entrainment problem during the movement process of high-speed landslide, well-documented landslide events have verified this phenomenon (Staron 2008). The landslide entrainment includes three main types: impact failure, scouring, and erosion (Pudasaini and Miller 2013). Using a small-scale physical models (linear scale of 1:10^4), Dufresne (2012) found that substrates are failing by the effect of upper sliding masses due to low internal and basal frictional resistance and then turn into the active basal sliding layer, increasing basal boundary roughness of erodible, deformable substrates resulting in shorter runout and longer deposits (decreased mobility of sliding mass). Using laboratory tests, Shea and van Wyk de Vries (2008) found that, in the presence of a substrate, the granular flow was slowed and "contraction-

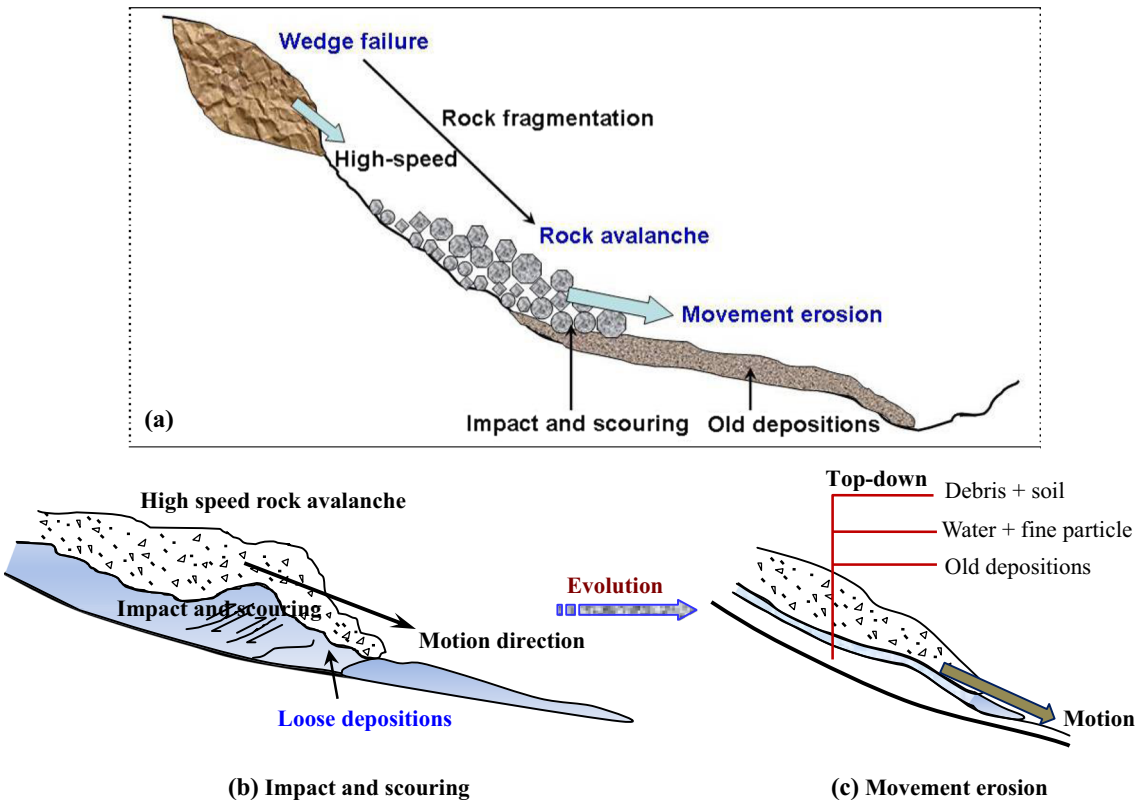

Fig. 17 Dynamic process of the movement of the 2000 Yigong landslide: **a** scheme of whole landslide process, **b** impact and scouring of bed materials by the high-speed rock avalanche, and **c** erosion of bed materials erosion the motion of debris avalanche

generated surface ridges" formed due to a lack of flow spreading, while the substrate itself was bulldozed at the flow front. According to the round top (RT) rock avalanche deposit, using field investigations and laboratory tests, Dufresne et al. (2010) found that the volume increase from the initial source volume to that of the final deposit existed because of the substrate entrainment during mass movement process, and the substrate entrainment increases the mobility of the avalanche mass by introducing significant quantities of water. Entrainment of bed deposits by surface water or sliding masses can lead to the change of motion behavior, such that the bed deposits on the steep slope entrainment by surface water can transform a dry rock/debris avalanche into debris flows, leading to greater areas affected and longer-runout distances covered (e.g., Kerle and vanWyk de Vries 2001; Evans et al. 2001). For the 2000 Yigong landslide, bed deposit entrainment by surface water and sliding masses transforms the rock avalanche into more mobile debris avalanche. However, the entrainment of landslide is a dynamical process, and its mechanical mechanism is very complicated and involves multiple areas of expertise: geotechnical engineering, hydromechanics, kinematics, and others. It is hard to present a theoretical model to describe the entrainment problem during the landslide motion process, and also, numerical simulations cannot be true representations of the entrainment process of landslides. However, the existence of water flow during the landslide process can aggravate the entrainment of landslides.

Conclusion

In this paper, the 2000 Yigong catastrophic landslide is taken as the study example, and the initiation mechanism and entrainment process of landslide are analyzed through field investigation, theoretical analysis, and laboratory tests. Some useful conclusions are presented here.

For the initiation mechanism of the 2000 Yigong landslide, the special geological conditions at the top slope provide precedent conditions for the initiation of landslide. The reasons for the initiation of the 2000 Yigong landslide are the coupling of long-term effects and short-term impact. For the long-tern effects, there are two aspects as mentioned above: (a) the loading-unloading cycle on the rock masses or structural surfaces due to the melting and freezing of glaciers and (b) the continuous seasonal and daily freeze-thaw cycles on the rock masses or structural surfaces. For the short-tern effects, the rising temperature on April 2000 accelerated the melting of glacier and snow, by coupling with the heavy rainfall, resulting in the decrease of shear strength and the increase of pore water pressure on the structural surfaces.

For the entrainment process of the 2000 Yigong landslide, the dynamical process can be summarized as follows: landslide initiation (wedge failure)→acceleration and fragmentation→rock avalanche→scouring and entrainment→debris avalanche→landslide deposition. There are three types of entrainment modes for the high-speed landslide: impact, scouring, and erosion. During the motion process of rock avalanche, the shear strength of bed material is decreased, excess pore water pressure is formed, and many bed deposits are impacted and scoured by the sliding mass. The landslide volume is gradually increased by the entrainment effect and resulted in the volume amplification of landslide. The existence of water flow plays a key role during the initiation and motion process of landslides.

Acknowledgments

We gratefully acknowledge the support of the National Natural Science Foundation of China (41472272, 41030742, and 41102194) and the Science Foundation for Excellent Youth Scholars of Sichuan University (2013SCU04A07). Dr. Gong-dan Zhou and Dr. Zhi-man Su provided valuable discussion on the initiation mechanism of the Yigong landslide. Critical comments by the reviewers greatly improved the initial manuscript.

References

Acharya G, Cochrane T, Davies T, Bowman E (2011) Quantifying and modeling post-failure sediment yields from laboratory-scale soil erosion and shallow landslide experiments with silty loess. Geomorphology 129:49–58

Angeli MG, Bunma J, Gasparetto P, Pasuto A (1998) A combined hillslope hydrology/stability model for low-gradient clay slopes in the Italian Dolomites. Eng Geol 49:1–13

Barth NC (2014) The Cascade rock avalanche: implications of a very large Alpine Fault-triggered failure, New Zealand. Landslides 11:327–341

Bayard D, Stähli M, Parriaux A, Flühler H (2005) The influence of seasonally frozen soil on the snowmelt runoff at two Alpine sites in southern Switzerland. J Hydrol 309:66–84

Borgatti L, Soldati M (2010) Landslides as a geomorphological proxy for climate change: a record from the Dolomites (northern Italy). Geomorphology 120:56–64

Cepeda J, Chávez JA, Martínez CC (2010) Procedure for the selection of runout model parameters from landslide back-analyses: application to the Metropolitan Area of San Salvador, El Salvador. Landslides 7:105–116

Crosta GB, Imposimato S, Roddeman D, Chiesa S, Moia (2005) Small fast-moving flow-like landslides in volcanic deposits: the 2001 Las Colinas Landslide (El Salvador). Eng Geol 79:185–214

Crosta GB, Imposimato S, Roddeman D (2009) Numerical modelling of entrainment/deposition in rock and debris-avalanches. Eng Geol 109:135–145

Dai FC, Tu XB, Xu C, Gong QM, Yao X (2011) Rock avalanches triggered by oblique-thrusting during the 12 May 2008 Ms 8.0 Wenchuan earthquake, China. Geomorphology 132:300–318

Draebing D, Krautblatter M, Diakau R (2014) Interaction of thermal and mechanical processes in steep permafrost rock walls: a conceptual approach. Geomorphology 226:226–235

Dufresne A (2012) Granular flow experiments on the interaction with stationary runout path materials and comparison to rock avalanche events. Earth Surf Process Landf 37:1527–1541

Dufresne A, Davies TR (2009) Longitudinal ridges in mass movement deposits. Geomorphology 105:171–181

Dufresne A, Davies TR, McSaveney MJ (2010) Influence of runout-path material on emplacement of the Round Top rock avalanche, New Zealand. Earth Surf Process Landf 35:190–201

Evans SG, Hungr O, Clague JJ (2001) Dynamics of the 1984 rock avalanche and associated distal debris flow on Mount Cayley, British Columbia, Canada; implications for landslide hazard assessment on dissected volcanoes. Eng Geol 61:29–51

Hsü KJ (1978) Albert Heim: observations on landslides. In: Voight B (ed) Rockslides and avalanches, vol 1. Elsevier, Amsterdam, pp 70–93

Hu M, Chen Q, Wang F (2009a) Experimental study on formation of Yigong long-distance high-speed landslide. Chin J Rock Mech Eng 28:138–143 (in Chinese)

Hu M, Wang F, Chen Q (2009b) Formation of tremendous Yigong landslide based on high-speed shear test. Chin J Geotech Eng 31:1602–1606 (in Chinese)

Huang RQ, Li WL (2009) Analysis of the geo-hazards triggered by the 12 May 2008 Wenchuan earthquake, China. Bull Eng Geol Environ 68:363–371

Hungr O, Corominas J, Eberhardt E (2005) Estimating landslide motion mechanism, travel distance and velocity. In: Proceedings of the International Conference on Landslide Risk Management, pp. 99–128

Kerle N, van Wyk de Vries B (2001) The 1998 debris avalanche at Casita volcano, Nicaragua—investigation of structural deformation as the cause of slope instability using remote sensing. J Volcanol Geotherm Res 105:49–63

Korup O, Clague JJ, Hermanns RL, Hewitt K, Strom A, Weidinger JT (2007) Giant landslides, topography, and erosion. Earth Planet Sci Lett 261:578–589

Krautblatter M, Funk D, Günzel FK (2013) Why permafrost rocks become unstable: a rock–ice-mechanical model in time and space. Earth Surf Process Landf 38:876–887

Kuo Y, Tsai Y, Chen Y, Shieh C, Miyamoto K, Itoh T (2013) Movement of deep-seated rainfall-induced landslide at Hsiaolin Village during Typhoon Morakot. Landslides 10:191–202
Lai Y, Yang Y, Chang X, Li S (2010) Strength criterion and elastoplastic constitutive model of frozen silt in generalized plastic mechanics. Int J Plast 26:1461–1484
Legros F (2002) The mobility of long-runout landslides. Eng Geol 63:301–331
Liu W (2002) Study on the characteristics of huge scale-super high speed-long distance landslide chain in Yigong, Tibet. Chin J Geol Hazard Control 13:9–18 (in Chinese)
Lo C, Lin M, Tang C, Hu J (2011) A kinematic model of the Hsiaolin landslide calibrated to the morphology of the landslide deposit. Eng Geol 123:22–39
Lv J, Wang Z, Zhou C (2003) Discussion on the occurrence of Yigong landslide in Tibet. Earth Sci J China Univ Geosci 28:107–110 (in Chinese)
Ma W, Wu Z, Zhang L, Chang X (1999) Analyses of process on the strength decrease in frozen soils under high confining pressures. Cold Reg Sci Technol 29:1–7
Mather AE, Hartley AJ, Griffiths (2014) The giant coastal landslides of Northern Chile: tectonic and climate interactions on a classic convergent plate margin. Earth Planet Sci Lett 388:249–256
McDougall S, Hungr O (2005) Dynamic modelling of entrainment in rapid landslides. Can Geotech J 42:1437–1448
Niemi NA, Oskin M, Burbank DW, Heimsath AM, Gabet EJ (2005) Effects of bedrock landslides on cosmogenically determined erosion rates. Earth Planet Sci Lett 237:480–498
Pudasaini SP, Miller SA (2013) The hypermobility of huge landslides and avalanches. Eng Geol 157:124–132
Sassa K (2000) Mechanism of flows in granular soils. In: Proceedings of GeoEng2000, Melbourne, 19–24 November, vol. 1. Technomic Publishing Company, USA, pp 1671–1702
Scott KM, Vallance JW, Kerle N, Macías JL, Strauch W, Devoli G (2005) Catastrophic precipitation-triggered lahar at Casita volcano, Nicaragua: occurrence, bulking and transformation. Earth Surf Process Landf 30:59–79
Shang Y, Yang Z, Li L, Liu D, Liao Q, Wang Y (2003) A super-large landslide in Tibet in 2000: background, occurrence, disaster, and origin. Geomorphology 54:225–243
Shang Y, Park H, Yang Z, Yang J (2005) Distribution of landslides adjacent to the northern side of the Yarlu Tsangpo Grand Canyon in Tibet, China. Environ Geol 48:721–741
Shea T, van Wyk de Vries B (2008) Structural analysis and analogue modelling of the kinetics and dynamics of rockslide avalanches. Geosphere 4:657–686
Staron L (2008) Mobility of long-runout rock flows: a discrete numerical investigation. Geophys J Int 172:455–463
Tang CL, Hu JC, Lin ML, Angelier J, Lu CY, Chan YC, Chu HT (2009) The Tsaoling landslide triggered by the Chi-Chi earthquake, Taiwan: insights from a discrete element simulation. Eng Geol 106:1–19
Tang H, Jia G, Hu X, Li D, Xiong C (2010) Characteristics of landslides induced by the great Wenchuan earthquake. J Earth Sci 21:104–113
Tsou C, Feng Z, Chigira M (2011) Catastrophic landslide induced by Typhoon Morakot, Shiaolin, Taiwan. Geomorphology 127:166–178
Van Wyk de Vries B, Self S, Francis PW, Keszthelyi L (2001) A gravitational spreading origin for the Socompa debris avalanche. J Volcanol Geotherm Res 105:225–247
Wang G, Sassa K, Fukuoka H (2003) Downslope volume enlargement of a debris slide–debris flow in the 1999 Hiroshima, Japan, rainstorm. Eng Geol 69:309–330
Wang G, Huang R, Chigira M, Wu X, Lourenço SDN (2013) Landslide amplification by liquefaction of runout-path material after the 2008 Wenchuan (M 8.0) earthquake, China. Earth Surf Process Landf 38:265–274
Weidinger JT, Korup O, Munack H, Altenberger U, Dunning SA, Tippelt G, Lottermoser W (2014) Giant rock slides from the inside. Earth Planet Sci Lett 389:62–73
Xu Q, Shang Y, van Asch T, Wang S, Zhang Z, Dong X (2012) Observations from the large, rapid Yigong rock slide—debris avalanche, southeast Tibet. Can Geotech J 49:589–606
Yin Y (2011) Recent catastrophic landslides and mitigation in China. J Rock Mech Geotech Eng 3:10–18
Yin Y, Xing A (2012) Aerodynamic modeling of the Yigong gigantic rock slide-debris avalanche, Tibet, China. Bull Eng Geol Environ 71:149–160
Yin Y, Zheng W, Li X, Sun P, Li B (2011) Catastrophic landslides associated with the M8.0 Wenchuan earthquake. Bull Eng Geol Environ 70:15–32
Zhou JW, Xu WY, Yang XG, Shi C, Yang ZH (2010) The 28 October 1996 landslide and analysis of the stability of the current Huashiban slope at the Liangjiaren Hydropower Station, Southwest China. Eng Geol 114:45–56
Zhou JW, Cui P, Fang H (2013a) Dynamic process analysis for the formation of Yangjiagou landslide-dammed lake triggered by the Wenchuan earthquake, China. Landslides 10:331–342
Zhou JW, Cui P, Yang XG (2013b) Dynamic process analysis for the initiation and movement of the Donghekou landslide-debris flow triggered by the Wenchuan earthquake. J Asian Earth Sci 76:70–84
Zhu P, Wang C, Tang B (2000) The deposition characteristic of supper debris flow in Tibet. J Mt Sci 18:453–456 (in Chinese)
Zhu Z, Ling X, Wang Z, Lu Q, Chen S, Zou Z, Guo Z (2011) Experimental investigation of the dynamic behavior of frozen clay from the Beiluhe subgrade along the QTR. Cold Reg Sci Technol 69:91–97

J.-w. Zhou (✉)
State Key Laboratory of Hydraulics and Mountain River Engineering,
Sichuan University,
Chengdu, Sichuan 610065, People's Republic of China
e-mail: jwzhou@scu.edu.cn

P. Cui
Key Laboratory of Mountain Hazards and Earth Surface Processes,
Chinese Academy of Science,
Chengdu, Sichuan 610044, People's Republic of China

M.-h. Hao
College of Water Resources and Hydropower,
Sichuan University,
Chengdu, Sichuan 610065, People's Republic of China